produce the hyperfine parameters of Cu(II) complexes with $d_{x^2-y^2}$ ($d_{z^2-x^2}$, $d_{y^2-z^2}$) ground states. However, the hyperfine parameters found in the complexes under consideration (Table V) are not in accord with $\kappa = 0.43$. From the experimental A_z and A_x values the κ and α parameters of Table V are estimated if the calculated φ angles are used and A_z and A_x have positive and negative signs, respectively. The depression of κ is directly correlated with a participation of the metal 4s orbital in the ground state, which is expected to have an effect opposite in sign to that of the polarized core electrons.[22]

A critical review of the calculated φ angles (140 ± 6°), κ values (0.22 ± 0.02), and α coefficients (0.93 ± 0.01) for the static limits listed in Table V imposes the need of small adjustments. The ligand field spectra show two broad transitions at 6500 ± 400 and 13 900 ± 100 cm^{-1} (Tables I and II), which can be assigned to the three symmetry-allowed transitons in he C_{2v} point group: $_a{}^2A_1$ ($\approx z^2 - y^2$) → $_b{}^2A_1$ ($\approx x^2$) and → $^2B_2$ (yz), $^2B_1$ (xz) (see previous section). The symmetry-forbidden transition $_a{}^2A_1 \rightarrow {}^2A_2$ (xy) is not observed but calculated to occur at about 13 000 cm^{-1}. This would imply a nonequivalence of the orbital contributions with $u_z > u_x \approx u_y$—in contrast to our earlier assumption of identical u_l contributions—and raises the angular parameters φ by about 5°, which on the other hand changes κ to 0.24 ± 0.02 and lowers α by about 0.01. An additional slight decrease of α has to be taken into account, because the equatorial Cu-N bond lengths deviate from the molecular x and y directions (Figure 2). The resulting α values of 0.91 (1) are larger than those that have been reported for the CuN_6 polyhedra in $Cu(TACN)_2^{2+}$ (TACN = 1,4,7-triazacyclononane)[24] and in hexanitro complexes[25] with $d_{x^2-y^2}$ ($d_{z^2-y^2}$) ground states ($\alpha = 0.87$). Possibly this is partly due to the $d_x{}^2$ admixture to the $d_{z^2-y^2}$ ground state, which is about 10 ± 3% for the compounds of Table V. Indeed the CoN_6 polyhedra in low-spin $Co(TACN)_2^{2+}$, which exhibit Jahn-Teller effects of comparable strength to that of Cu^{2+} but possess $d_z{}^2$ ($d_x{}^2$) ground states, have much larger α coefficients ($\alpha = 0.93$) than those of the just mentioned CuN_6 polyhedra in the same coordination. The calculated κ value (≈0.24) allows one to estimate the fractional occupancy of the 4s orbital by the unpaired electron.[23,26] The amount of 2.8% reasonably compares with the 4.5% calculated for the just mentioned $Co(TACN)_2^{2+}$ complex.[24]

Acknowledgment. We wish to acknowledge financial support by the Comision Interministerial de Ciencia y Tecnologia and the Fonds der Chemischen Industrie. The receipt of a research fellowship for a postdoctoral stay in Marburg from the Generalitat Valenciana is gratefully acknowledged by J.-V.F.

Supplementary Material Available: Table SI (complete crystallographic data) and Table SII (anisotropic thermal parameters of all atoms besides hydrogen; atomic positions and isotropic thermal parameters for hydrogen) (4 pages); Table SIII (observed and calculated structure factors) (7 pages). Ordering information is given on any current masthead page.

(22) McGarvey, B. R. *J. Phys. Chem.* **1967**, *71*, 51.
(23) Hitchman, M. A.; McDonald, R. G.; Reinen, D. *Inorg. Chem.* **1986**, *25*, 519.
(24) Reinen, D.; Ozarowski, A.; Jakob, B.; Pebler, J.; Stratemeier, H.; Wieghardt, K.; Tolksdorf, I. *Inorg. Chem.* **1987**, *26*, 4010.
(25) Ozarowski, A.; Reinen, D. *Inorg. Chem.* **1985**, *24*, 3860.
(26) Morton, J. R.; Preston, K. F. *J. Magn. Reson.* **1978**, *30*, 577.

Contribution from the Department of Inorganic Chemistry, University of Barcelona, Diagonal 647, 08028-Barcelona, Spain, Laboratoire de Chimie Inorganique, URA No. 420, Université de Paris-Sud, 91405 Orsay, France, and Laboratoire de Chimie de Coordination du CNRS, UP No. 8241, 205 route de Narbonne, 31077 Toulouse, France

Structure and Magnetic and Spectroscopic Properties of a $Ni^{II}Cu^{II}Ni^{II}$ Trinuclear Species

Juan Ribas,*[1a] Carmen Diaz,[1a] Ramon Costa,[1a] Yves Journaux,[1b] Corine Mathoniere,[1b] Olivier Kahn,*[1b] and Alain Gleizes[1c]

Received September 6, 1989

The two compounds of formula $\{[Ni(bapa)(H_2O)]_2Cu(pba)\}(ClO_4)_2$ and $[Ni(bapa)(H_2O)Cu(pba)]\cdot 2H_2O$, hereafter abbreviated as [NiCuNi] and [NiCu], respectively, have been synthesized. bapa is bis(3-aminopropyl), and pba is 1,3-propylenebis(oxamato). The crystal structure of [NiCuNi] has been solved. It crystallizes in the orthorhombic system, space group $Pna2_1$, with a = 9.826 (2) Å, b = 12.793 (1) Å, c = 27.266 (3) Å, and Z = 4. The structure consists of $Ni^{II}Cu^{II}Ni^{II}$ trinuclear cations and noncoordinated perchlorate anions. The nickel atoms are in a distorted octahedral environment, and the copper atom is in an environment markedly distorted from square planar to tetrahedral. The central copper atom is bridged to the terminal nickel atoms by oxamato groups with Cu···Ni separations of 5.305 (2) and 5.326 (2) Å. The magnetic properties of both compounds have been investigated. The $\chi_M T$ versus T plot (χ_M is the molar magnetic susceptibility and T the temperature) for [NiCuNi] exhibits the minimum characteristic for this kind of polymetallic species with an irregular spin state structure. The Ni(II)-Cu(II) isotropic interaction parameter was found to be $J = -90.3$ cm^{-1} ($H = -JS_{Ni} \cdot S_{Cu}$). The powder EPR spectrum at 10 K is poorly resolved. It shows a broad signal corresponding to the envelope of the two Kramers doublets arising from the spin-quartet ground state. The $\chi_M T$ versus T plot for [NiCu] is typical of an antiferromagnetically coupled pair with a spin-doublet ground state and a doublet-quartet energy gap equal to $3J/2 = -141.9$ cm^{-1}. The electronic spectra of [NiCuNi] has also been investigated. It shows a triplet → singlet spin-forbidden transition associated with the nickel(II) ion and activated by an exchange mechanism.

Introduction

We have recently pointed out that it was possible to stabilize a state of high-spin multiplicity in a polymetallic entity without imposing ferromagnetic interactions between nearest neighbor magnetic centers.[2,3] The strategy for this consists of aligning two high local spins along the same direction owing to antiferromagnetic interactions with a small local spin located between them. The basic scheme for describing the ground state of a trinuclear species of this kind is

(1) (a) University of Barcelona. (b) Université de Paris-Sud. (c) Laboratoire de Chimie de Coordination du CNRS. Present address: ENSCT, URA No. 445, 118 route de Narbonne, 31077 Toulouse, France.
(2) Pei, Y.; Journaux, Y.; Kahn, O. *Inorg. Chem.* **1988**, *27*, 399.
(3) Kahn, O. *Struct. Bonding (Berlin)* **1987**, *68*, 89.
(4) Verdaguer, M.; Julve, M.; Michalowicz, A.; Kahn, O. *Inorg. Chem.* **1983**, *22*, 2624.
(5) Drillon, M.; Gianduzzo, J. C.; Georges, R. *Phys. Lett.* **1983**, *96A*, 413.
(6) Gleizes, A.; Verdaguer, M. *J. Am. Chem. Soc.* **1984**, *106*, 3727.
(7) Beltran, D.; Escriva, E.; Drillon, M. *J. Chem. Soc., Faraday Trans. 2* **1982**, *78*, 1773.
(8) Coronado, E.; Drillon, M.; Fuertes, A.; Beltran, D.; Mosset, A.; Galy, J. *J. Am. Chem. Soc.* **1986**, *108*, 900.
(9) Pei, Y.; Verdaguer, M.; Kahn, O.; Sletten, J.; Renard, J. P. *Inorg. Chem.* **1987**, *26*, 138.

0020-1669/90/1329-2042$02.50/0 © 1990 American Chemical Society

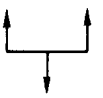

In some way, the small central spin polarizes the two high terminal spins in a ferromagnetic-like fashion. The spin-state structure of such a compound is said to be irregular in the sense where the spin associated with the low-lying states does not vary in a monotonical fashion versus the energy. Rather, when going down in energy, the spin first decreases and then increases. Such a behavior is revealed by the $\chi_M T$ versus T plot, χ_M being the molar magnetic susceptibility and T the temperature. This plot exhibits a characteristic minimum, which may be interpreted as follows: In the high-temperature limit, when kT is much larger than the absolute value of the exchange parameter $|J|$, $\chi_M T$ is equal to the sum of the local contributions. When the temperature is decreased, the first state to be thermally depopulated is obviously that of highest energy. This state has the highest spin; all the local spins are aligned along the same direction. It follows that $\chi_M T$ decreases. In the low-temperature range now, only the ground state and the first excited states are significantly populated. When the temperature is decreased further, the states with a small spin are more and more depopulated in favor of states of lower energy with an higher spin, and $\chi_M T$ increases. The result from the decrease of $\chi_M T$ upon cooling down in the high-temperature range and from its increase in the low-temperature range is that the $\chi_M T$ versus T should exhibit a minimum. This minimum may occur for ABA trinuclear species with local spins $2S_A > S_B + {}^1/_2$ and for $(AB)_n$ alternating ring chains with $S_A \neq S_B$ as well.[3,10]

So far, a $Mn^{II}Cu^{II}Mn^{II}$ trinuclear compound and a $Ni^{II}Cu^{II}Ni^{II}$ trinuclear compound displaying the magnetic behavior described above have been reported.[2] They were synthesized from the reaction of the copper(II) precursor $[Cu(pba)]^{2-}$ with $[M(Me_6\text{-}[14]ane\text{-}N_4)]^{2+}$, M being Mn or Ni and Me_6-[14]ane-N_4 being (±)5,7,7,12,14,14-hexamethyl-1,4,8,11-tetraazacyclotetradecane. For neither of these two compounds was a single crystal suitable for X-ray work obtained. Isolated $Fe^{III}Cu^{II}Fe^{III}$ units in an extended lattice with an usovite-like structure has also been reported.[11,12] Along the same line, an elegant spectroscopic study dealing with a $Mn^{II}Ti^{II}Mn^{II}$ triad in $MgCl_2$ has recently been published.[13] This triad shows the kind of spin state structure pointed out above.

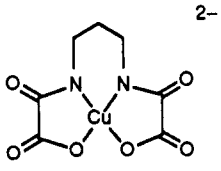

$[Cu(pba)]^{2-}$

In this paper, we report on a new $Ni^{II}Cu^{II}Ni^{II}$ species. Its formula is $\{[Ni(bapa)(H_2O)]_2Cu(pba)\}(ClO_4)_2$, bapa standing for bis(3-aminopropyl)amine. We successively describe the synthesis of this compound, hereafter abbreviated by [NiCuNi], its crystal structure, and its magnetic and spectroscopic properties. In the course of the synthesis of [NiCuNi], we obtained another compound, namely the neutral binuclear species $\{[Ni(bapa)(H_2O)]Cu(pba)\}\cdot 2H_2O$, hereafter abbreviated by [NiCu]. We also report here on the magnetic properties of [NiCu].

Experimental Section

Syntheses. The compound [NiCuNi] was prepared as follows: 0.13 g (10^{-3} mol) of bis(3-aminopropyl)amine was added with continuous stirring to a solution of 0.36 g (10^{-3} mol) of nickel perchlorate hexahydrate in 10 mL of water. A 0.21-g (0.5×10^{-3} mol) sample of sodium (1,3-propylenebis(oxamato))cuprate(II) hexahydrate[14,15] dissolved in 10 mL of hot water was then added slowly to the rapidly stirred solution. A slight blue precipitate of [NiCu] was removed by filtration, and the concentrated solution was allowed to cool down to room temperature. [NiCuNi] precipitated as a microcrystalline powder, which was filtered and dried under vacuum. [NiCuNi] is soluble in water and in acetonitrile with slow decomposition. Anal. Calcd for $C_{19}H_{44}N_8O_{16}Cl_2CuNi_2$: C, 25.57; H, 4.97; N, 12.55; Cl, 7.94; Cu, 7.12; Ni, 13.16. Found: C, 25.58; H, 4.96; N, 12.57; Cl, 8.13; Cu, 7.05; Ni, 13.06. Well-shaped single crystals were obtained by slow evaporation of the aqueous solution.

Working at room temperature and with more dilute solutions affords a larger amount of [NiCu]. This binuclear species is insoluble in any usual solvent, and we have not been able to get single crystals suitable for X-ray diffraction. Anal. Calcd for $C_{13}H_{29}N_5O_9CuNi$: C, 29.93; H, 5.60; Cu, 12.18; Ni, 11.25. Found: C, 29.71; H, 5.42; N, 13.31; Cu, 11.83; Ni, 10.88.

Crystal Data Collection and Refinement. A single crystal was mounted on a Enraf-Nonius CAD4 four-circle diffractometer. The crystallographic data, conditions retained for the intensity data collection, and some features of the structure refinement are listed in Table I. The accurate unit-cell constants were determined from the least-squares refinement of the setting angles of 25 reflections. They are listed in Table I along with some crystallographic experimental data; a more complete summary is in the supplementary material. The observed systematic extinctions were consistant with space groups *Pnma* and $Pna2_1$. The absence of 00z Harker peaks in the Patterson map showed the space group to be $Pna2_1$, that is, noncentrosymmetric. The refinement of the structure was performed by full-matrix least-squares techniques, starting with the positions of the metal atoms determined from the Patterson map, and using Fourier and difference-Fourier syntheses to locate the lighter atoms.[16]

All atoms except those of hydrogen and carbon were refined anisotropically. The carbon atoms were refined isotropically. The hydrogen atoms, except those linked to two nitrogen atoms and those belonging to the disordered propylene chains (vide infra), were introduced as fixed contributors at positions read in difference-Fourier maps. They were given isotropic thermal parameters equal to the equivalent B of the atoms to which they were attached. In the last cycle of refinement on F_o (2198 observations with $I > \sigma(I)$, 337 variables), the highest (variable shift)/esd ratio was 0.5. The final agreement factors are in Table I. The subsequent difference-Fourier map showed no significant peak.

The refined positional parameters and equivalent or actual B's for non-hydrogen atoms are listed in Table II. The central carbon atom of the propylene chain joining two oxamato groups was found to be equally distributed over two positions (C3a and C3b). The oxygen atoms of the perchlorate anion p2 were also found distributed over two sets of positions, the one with a 60% occupancy (O1p2 → O4p2), the other one with a 40% occupancy (O5p2 → O8p2).

Magnetic Measurements. These were carried out with a Faraday type magnetometer equipped with a helium continuous-flow cryostat working in the 4.2–300 K temperature range. For both compounds [NiCuNi] and [NiCu], the independence of the magnetic susceptibility versus the applied field was checked at room temperature. Mercury tetrakis(thiocyanato)cobaltate was used as a susceptibility standard. Diamagnetic corrections were estimated as -423×10^{-6} cm^3 mol^{-1} for [NiCuNi] and -295×10^{-6} cm^3 mol^{-1} for [NiCu].

EPR Spectra. These were recorded on powder samples at X-band frequency with a Bruker ER 200D spectrometer equipped with an helium continuous-flow cryostat. The magnetic field was determined with a Hall

Table I. Crystallographic Data and Experimental Parameters for $\{[Ni(bapa)(H_2O)]_2Cu(pba)\}(ClO_4)_2$

formula	$(CuNi_2O_8N_8C_{19}H_{44})(ClO_4)_2$	space group	$Pna2_1$
		radiation, Å	λ(Mo Kα) = 0.7093
fw	892.47	d_{calcd}, g cm^{-3}	1.729
a, Å	9.826 (2)	μ, cm^{-1}	19.4
b, Å	12.793 (1)	abs cor	no
c, Å	27.266 (3)	R on F_o ($I > \sigma(I)$)	0.056
V, Å^3	3427		
Z	4	R_w on F_o ($I > \sigma(I)$)	0.059
temp, K	293		

(10) Kahn, O.; Pei, Y.; Verdaguer, M.; Renard, J. P.; Sletten, J. *J. Am. Chem. Soc.* **1988**, *110*, 782.
(11) Darriet, J.; Quiang, X.; Tressaud, A.; Hagenmuller, P. *Mat. Res. Bull.* **1986**, *21*, 1351.
(12) Darriet, J.; Quiang, X.; Tressaud, A. *C. R. Acad. Sci., Ser. 2* **1986**, *303*, 1545.
(13) Herren, M.; Jacobsen, S. M.; Güdel, H. U. *Inorg. Chem.* **1989**, *28*, 504.
(14) Nonoyama, K.; Ojima, H.; Nonoyama, M. *Inorg. Chim. Acta* **1976**, *20*, 127.
(15) Ojima, H.; Nonoyama, M. *Coord. Chem. Rev.* **1988**, *92*, 85.
(16) Computer: DEC VAX 11-730. Programs: SDP Structure Determination Package. Enraf-Nonius, Delft, The Netherlands, 1979. ORTEP. Report ORNL-3794, Oak Ridge National Laboratory: Oak Ridge, TN, 1965.

Table II. Positional Parameters and Equivalent *B*'s and their Estimated Standard Deviations for Non-H Atoms in $\{[Ni(bapa)(H_2O)]_2Cu(pba)\}(ClO_4)_2$

atom	*x*	*y*	*z*	B,[a] Å^2
Cu	0.2125 (2)	0.4214 (1)	1/4	2.65 (3)
Ni1	0.6552 (2)	0.4360 (1)	0.13889 (7)	2.22 (3)
Ni2	−0.2493 (2)	0.4344 (1)	0.35211 (7)	2.22 (3)
O1	0.3333 (9)	0.3182 (6)	0.2184 (3)	2.9 (2)
O2	0.0883 (8)	0.3209 (6)	0.2831 (3)	2.7 (2)
O11	0.5161 (8)	0.3225 (6)	0.1702 (3)	2.5 (2)
O21	0.5519 (8)	0.5256 (6)	0.1893 (3)	2.6 (2)
O12	−0.0916 (9)	0.3255 (6)	0.3326 (3)	2.7 (2)
O22	−0.1280 (8)	0.5308 (7)	0.3109 (3)	3.0 (2)
Ow1	0.8008 (8)	0.3886 (7)	0.1980 (4)	2.9 (2)
Ow2	−0.3522 (9)	0.3906 (7)	0.2881 (3)	3.1 (2)
N1	0.348 (1)	0.5220 (8)	0.2326 (5)	3.4 (2)
N2	0.078 (1)	0.5235 (8)	0.2717 (5)	3.3 (2)
N11	0.750 (1)	0.3211 (9)	0.0998 (4)	2.8 (2)
N21	0.779 (1)	0.5611 (8)	0.1207 (5)	3.5 (3)
N31	0.514 (1)	0.4775 (8)	0.0857 (4)	3.0 (2)
N12	−0.349 (1)	0.3129 (9)	0.3883 (4)	3.5 (3)
N22	−0.401 (1)	0.5464 (9)	0.3588 (5)	3.6 (3)
N32	−0.144 (1)	0.4892 (8)	0.4162 (4)	2.6 (2)
C1	0.344 (2)	0.636 (1)	0.2396 (6)	4.3 (3)*
C2	0.090 (2)	0.636 (1)	0.2640 (6)	4.0 (3)*
C3a	0.246 (3)	0.668 (2)	0.2756 (9)	2.9 (5)*
C3b	0.199 (3)	0.671 (2)	0.233 (1)	3.5 (6)*
C11	0.432 (1)	0.363 (1)	0.1972 (5)	2.6 (2)*
C21	0.451 (1)	0.4817 (9)	0.2069 (4)	2.1 (2)*
C31	0.726 (2)	0.309 (1)	0.0462 (6)	4.0 (3)*
C41	0.581 (2)	0.326 (1)	0.0344 (6)	4.6 (3)*
C51	0.537 (2)	0.437 (1)	0.0355 (6)	4.2 (3)*
C61	0.482 (2)	0.591 (1)	0.0825 (6)	4.2 (3)*
C71	0.608 (2)	0.658 (1)	0.0735 (6)	4.2 (3)*
C81	0.710 (2)	0.662 (1)	0.1156 (6)	4.1 (3)*
C12	−0.010 (1)	0.3669 (9)	0.3031 (5)	2.2 (2)*
C22	−0.023 (1)	0.483 (1)	0.2936 (5)	2.4 (2)*
C32	−0.353 (2)	0.308 (1)	0.4421 (6)	4.3 (3)*
C42	−0.213 (2)	0.331 (1)	0.4630 (6)	4.3 (3)*
C52	−0.172 (2)	0.445 (1)	0.4635 (6)	4.7 (3)*
C62	−0.137 (2)	0.604 (1)	0.4199 (7)	5.1 (4)*
C72	−0.277 (2)	0.654 (1)	0.4192 (7)	5.8 (4)*
C82	−0.355 (2)	0.651 (1)	0.3728 (7)	5.7 (4)*
Cl1	0.1155 (3)	0.4742 (3)	0.1140 (2)	3.41 (7)
Cl2	0.2526 (4)	0.4883 (3)	0.4150 (2)	5.9 (1)
O1p1	0.239 (1)	0.4171 (9)	0.1137 (6)	7.2 (4)
O2p1	0.024 (1)	0.431 (1)	0.0802 (5)	6.6 (3)
O3p1	0.143 (1)	0.5788 (9)	0.1021 (7)	8.5 (4)
O4p1	0.058 (1)	0.465 (1)	0.1613 (5)	7.5 (4)
O1p2	0.182 (2)	0.489 (2)	0.461 (1)	7.9 (6)*
O2p2	0.371 (2)	0.429 (2)	0.4257 (8)	6.7 (5)*
O3p2	0.156 (2)	0.439 (2)	0.3874 (8)	6.5 (5)*
O4p2	0.285 (3)	0.591 (3)	0.390 (1)	11.2 (9)*
O5p2	0.195 (5)	0.443 (3)	0.471 (2)	11 (1)*
O6p2	0.152 (5)	0.526 (3)	0.389 (2)	10 (1)*
O7P2	0.323 (4)	0.410 (3)	0.381 (2)	9 (1)*
O8P2	0.337 (3)	0.576 (2)	0.426 (1)	6.2 (7)*

[a] Starred values denote atoms that were refined isotropically. Values for anisotropically refined atoms are given in the form of the isotropic equivalent displacement parameter defined as $(4/3)[a^2B(1,1) + b^2B(2,2) + c^2B(3,3) + ab(\cos\gamma)B(1,2) + ac(\cos\beta)B(1,3) + bc(\cos\alpha)B(2,3)]$.

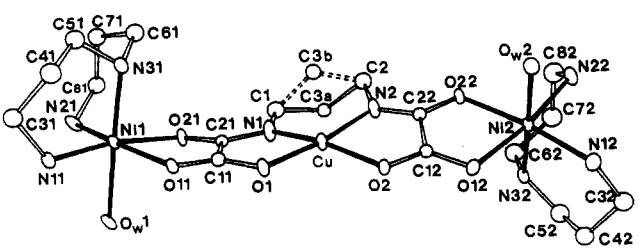

Figure 1. Perspective view of the trinuclear cation $\{[Ni(bapa)(H_2O)]_2Cu(pba)\}^{2+}$.

probe, and the klystron frequency, with a Hewlett-Packard frequency meter.

Table III. Selected Bond Lengths (Å) and Angles (deg) for $\{[Ni(bapa)(H_2O)]_2Cu(pba)\}(ClO_4)_2$

Around Cu			
Cu–O1	1.974 (9)	O1–Cu–O2	97.7 (3)
Cu–O2	1.988 (8)	O2–Cu–N2	83.1 (4)
Cu–N1	1.910 (11)	N2–Cu–N1	95.4 (4)
Cu–N2	1.948 (11)	N1–Cu–O1	85.6 (4)
Cu···Ni1	5.305 (2)	O1–Cu–N2	171.2 (5)
Cu···Ni2	5.326 (2)	O2–Cu–N1	167.3 (5)

Around Ni's		
	i = 1	*i* = 2
Ni*i*–O1*i*	2.170 (8)	2.150 (9)
Ni*i*–O2*i*	2.058 (9)	2.051 (9)
Ni*i*–Ow*i*	2.238 (9)	2.094 (9)
Ni*i*–N1*i*	2.041 (11)	2.082 (12)
Ni*i*–N2*i*	2.073 (10)	2.073 (11)
Ni*i*–N3*i*	2.074 (12)	2.148 (11)
O1*i*–Ni*i*–O2*i*	78.4 (3)	80.5 (3)
O1*i*–Ni*i*–Ow*i*	86.4 (3)	88.2 (3)
O1*i*–Ni*i*–N1*i*	90.7 (4)	88.4 (4)
O1*i*–Ni*i*–N2*i*	169.1 (4)	170.6 (5)
O1*i*–Ni*i*–N3*i*	91.5 (4)	93.7 (4)
O2*i*–Ni*i*–Ow*i*	89.2 (4)	89.1 (4)
O2*i*–Ni*i*–N1*i*	167.3 (4)	168.6 (4)
O2*i*–Ni*i*–N2*i*	91.1 (4)	92.8 (4)
O2*i*–Ni*i*–N3*i*	89.7 (4)	88.2 (4)
Ow*i*–Ni*i*–N1*i*	83.6 (4)	88.3 (4)
Ow*i*–Ni*i*–N2*i*	90.3 (4)	85.0 (4)
Ow*i*–Ni*i*–N3*i*	177.8 (4)	176.4 (4)
N1*i*–Ni*i*–N2*i*	99.3 (5)	98.0 (5)
N1*i*–Ni*i*–N2*i*	97.2 (5)	94.8 (5)
N2*i*–Ni*i*–N3*i*	91.6 (5)	92.7 (5)

Oxamido Bridge		
	i = 1	*i* = 2
C1*i*–O*i*	1.272 (16)	1.255 (14)
C1*i*–O1*i*	1.220 (16)	1.254 (14)
C2*i*–N*i*	1.339 (17)	1.275 (16)
C2*i*–O2*i*	1.234 (14)	1.287 (15)
C1*i*–C2*i*	1.548 (17)	1.511 (17)
N*i*–C*i*	1.467 (19)	1.455 (19)
C1–C3a	1.44 (3)	
C2–C3a	1.61 (3)	
C1–C3b	1.50 (3)	
C2–C3b	1.44 (3)	
Ni*i*–O1*i*–C1*i*	112.0 (8)	110.3 (7)
Ni*i*–O2*i*–C2*i*	113.6 (8)	112.2 (8)
O*i*–C1*i*–O1*i*	126.6 (12)	125.0 (11)
O*i*–C1*i*–C2*i*	117.3 (12)	116.9 (12)
O1*i*–C1*i*–C2*i*	116.1 (12)	117.9 (11)
N*i*–C2*i*–O2*i*	129.6 (12)	127.0 (13)
N*i*–C2*i*–C1*i*	112.0 (12)	114.4 (12)
O2*i*–C2*i*–C1*i*	118.4 (12)	118.4 (12)
Cu–N*i*–C*i*	128.0 (10)	124.3 (9)
Cu–N*i*–C2*i*	113.6 (9)	113.5 (9)
C*i*–N*i*–C2*i*	118.1 (12)	122.3 (12)
Cu–O*i*–C1*i*	110.8 (8)	111.5 (8)
N*i*–C*i*–C3a	113.2 (15)	107.5 (14)
N*i*–C*i*–C3b	108.2 (15)	117.2 (16)
C1–C3a–C2	115.3 (19)	
C1–C3b–C2	122.2 (21)	

Electronic Spectra. These were recorded with a Varian 2300 spectrophotometer in acetonitrile solution.

Description of the Structure of [NiCuNi]

The unit cell contains four trinuclear [NiCuNi] dications and two symmetrically independent sets of four perchlorate anions. Selected bond lengths and angles are listed in Table III. Other distances and angles, atom to mean-plane distances and dihedral angles will be found in the supplementary material. A view of the trinuclear unit with the atom-labeling scheme is presented in Figure 1, and a simplified side view, in Figure 2.

Both nickel atoms are in assymmetrical octahedral environment made of two oxalato oxygen atoms (O1*i*, O2*i*) and two nitrogen atoms (N1*i*, N2*i*) in equatorial positions and an amino nitrogen

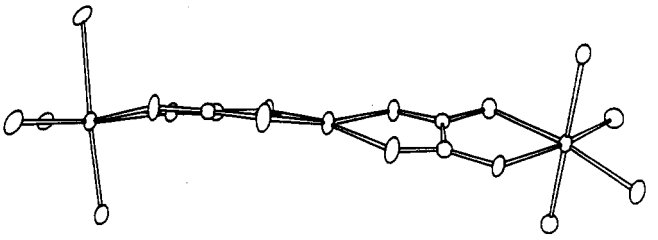

Figure 2. Side view of $\{[Ni(bapa)(H_2O)]_2Cu(pba)\}^{2+}$ emphasizing the pronounced distorsion of the CuN_2O_2 chromophore, from a square planar toward a tetrahedral environment.

atom (N3*i*) and a water oxygen atom (Ow*i*) in apical positions. The nickel atoms deviate by ca. 0.1 Å from the mean equatorial plane toward the apical nitrogen atoms, and either oxamato chelate displays Ni–O bond lengths that differ by ca. 0.1 Å (Ni1–O11 = 2.170 (8) Å and Ni1–O21 = 2.058 Å; Ni2–O12 = 2.150 (9) Å and Ni2–O22 = 2.051 (9) Å.

The N_2O_2 environment of the copper atom is markedly distorted from square planar to tetrahedral, resulting in atom to mean-plane distances of about 0.2 Å. The distorsion can be evaluated through the distorsion parameter Δ introduced by Galy et al.[17] from the dihedral angles according to

$$\Delta = \frac{720 - (\delta_1 + \delta_2 + \delta_3 + \delta_4)}{423} + \frac{\delta_5 + \delta_6}{657} \qquad (1)$$

where the δ_i's are dihedral angles defined as follows:

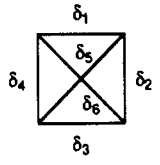

Δ is then found equal to 20%. The planes defined by atoms Cu, N1, and O1 on one hand and Cu, N2, and O2 on the other hand make an angle of 16°. Besides this torsion, either equatorial moity markedly deviates from planarity through the conjugate effects of (i) the deviations of the nickel atoms from their equatorial plane of coordination, (ii) the dihedral angles between planes defined by Ni*i*, O1*i*, and O2*i* and O1*i*, C1*i*, C2*i*, and O2*i* (10° for $i = 1$; 4° for $i = 2$), (iii) the torsion angles of the oxamato bridges around their C–C bonds (6° for $i = 1$; 10° for $i = 2$), and (iv) the dihedral angles between planes defined by Cu, O*i*, and N*i* and N*i*, O*i*, C1*i*, and C2*i* (5° for $i = 1$; 1° for $i = 2$) (see Figure 2).

Intramolecular separations between metal ions are Cu···Ni1 = 5.305 (2) Å and Cu···Ni2 = 5.326 (2) Å. The shortest intermolecular separation is Cu···Ni2 = 5.349 Å. Intermolecular hydrogen bonding involving amino and water hydrogen atoms on one hand, and perchlorato and oxamato oxygen atoms on the other hand is present and is summarized in the supplementary material.

Magnetic Properties

[NiCuNi]. The $\chi_M T$ versus T plot for [NiCuNi] is shown in Figure 3. It exhibits the expected minimum. At 290 K, $\chi_M T$ is equal to 2.31 cm^3 K mol^{-1}, smoothly decreases upon cooling, reaches the minimum around 100 K with $\chi_M T$ = 2.03 cm^3 K mol^{-1} and increases upon cooling further. At 4.2 K, $\chi_M T$ is equal to 2.20 cm^3 K mol^{-1}. It is important to point out that this magnetic curve is weakly contrasted, the two extreme values of $\chi_M T$ being 2.31 and 2.03 cm^3 K mol^{-1}, respectively, so that one cannot expect an accurate determination of the spin Hamiltonian parameters. If the very weak difference between the two Ni–Cu moities in [NiCuNi] is neglected, this Hamiltonian may be written as

$$\mathbf{H} = -J(S_{Ni1}\cdot S_{Cu} + S_{Ni2}\cdot S_{Cu}) + D[S_z^2 - \tfrac{1}{3}S(S+1)]\delta_{S,3/2}\delta_{S',2} + \beta H[g_{Ni}(S_{Ni1} + S_{Ni2}) + g_{Cu}S_{Cu}] \qquad (2)$$

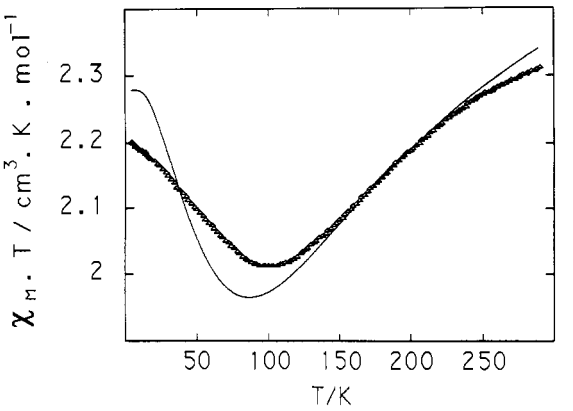

Figure 3. $\chi_M T$ versus T plot for $\{[Ni(bapa)(H_2O)]_2Cu(pba)\}(ClO_4)_2$: (Δ) experimental points; (–) calculated curve.

where an axial zero-field splitting parameter within the quartet ground state is taken into account, the corresponding parameter being D. The energy gap between the two Kramers doublets $\pm^3/_2$ and $\pm^1/_2$ arising from the spin quartet ground state is $2D$. The spectrum of the low-lying spin states deduced from (2) is shown in Figure 4, in the form of the energy versus spin diagram. Each state is represented by an arrow of which the length is equal to the spin associated with this state. The states have been labeled by idealizing the molecular symmetry in D_{2h}, which would be correct if the site symmetry of copper was strictly D_{2h} and that of nickel strictly C_{2v}. In Figure 4, we have also indicated the relations between molecular $g_{S,S'}$ and local g_{Ni} and g_{Cu} Zeeman factors.[2,18,19] The S and S' operators are defined by

$$S' = S_{Ni1} + S_{Ni2}$$
$$S = S' + S_{Cu} \qquad (3)$$

The parallel and perpendicular molar magnetic susceptibilities deduced from (2) are then

$$\chi_{M\parallel} = (N\beta^2/4kT)\{g_{3/2,2}^2[9\exp(-D/kT) + \exp(D/kT)] + g_{1/2,1}^2\exp(J/2kT) + g_{1/2,0}^2\exp(3J/2kT) + 10g_{3/2,1}^2\exp(2J/kT) + 35g_{5/2,2}^2\exp(5J/2kT)\}/\{\exp(-D/kT) + \exp(D/kT) + \exp(J/2kT) + \exp(3J/2kT) + 2\exp(2J/kT) + 3\exp(5J/2kT)\} \qquad (4)$$

$$\chi_{M\perp} = (N\beta^2/4kT)\{g_{3/2,2}^2[-(3kT/D)\exp(-D/kT) + (4 - 3kT/D)\exp(D/kT)] + g_{1/2,1}^2\exp(J/2kT) + g_{1/2,0}^2\exp(3J/2kT) + 10g_{3/2,1}^2\exp(2J/kT) + 35g_{5/2,2}^2\exp(5J/2kT)\}/\{\exp(-D/kT) + \exp(D/kT) + \exp(J/2kT) + \exp(3J/2kT) + 2\exp(2J/kT) + 3\exp(5J/2kT)\} \qquad (5)$$

In (2) and (4) and (5), it has been assumed that the local g factors were isotropic and that the spin states did not couple through the local anisotropy of the Ni(II) ion, $(|J| \gg |D|)^2$.

The least-squares fitting of the experimental data is weakly sensitive to the value of D, which consequently cannot be determined from the magnetic data. The other parameters are found as $J = -90.3$ cm^{-1}, $g_{Ni} = 2.19$, and $g_{Cu} = 2.12$. The agreement factor R defined as $\sum[(\chi_M T)^{obs} - (\chi_M T)^{calc}]^2/\sum[(\chi_M T)^{obs}]^2$ is then equal to 3.5×10^{-3}. Such an agreement is not excellent, as can be seen in Figure 3. In particular, the magnetic data below about 30 K are not well reproduced. Experimental and calculated data are listed in the supplementary material.

The X-band powder EPR spectrum of [NiCuNi] at 10 K presents a very broad signal covering the whole 0–6000-G field range with a well-defined maximum around 1600 G and a smooth

(17) Galy, J.; Bonnet, J. J.; Anderson, S. *Acta Chem. Scand., Ser. A* **1979**, *A33*, 383.

(18) Scaringe, R. P.; Hodgson, D.; Hatfield, W. E. *Mol. Phys.* **1978**, *35*, 701.

(19) Gatteschi, D.; Bencini, A. In *Magneto-Structural Correlation in Exchange Coupled Systems*; Willett, R. D., Gatteschi, D., Kahn, O., Eds.; D. Reidel: Dordrecht, The Netherlands, 1985; p 241.

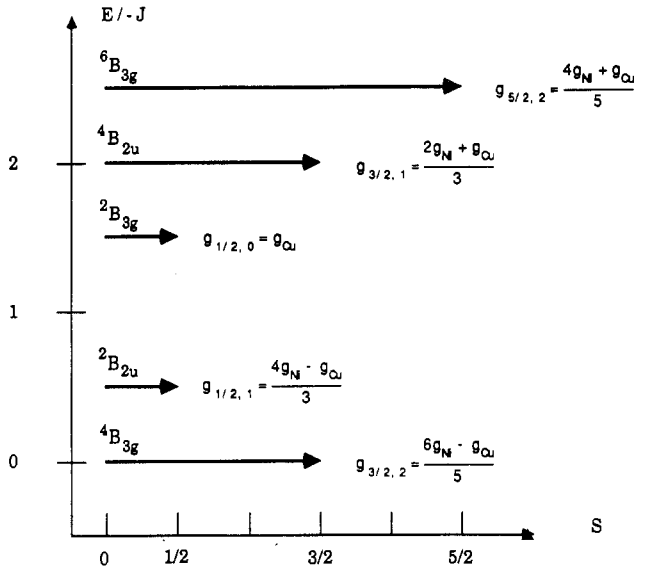

Figure 4. Energy versus spin diagram for the low-lying state of [NiCuNi]. The symmetry labels refer to an idealized D_{2h} molecular symmetry. For each state is indicated the relation between molecular $g_{S,S'}$ and local g_{Ni} and g_{Cu} factors (see text).

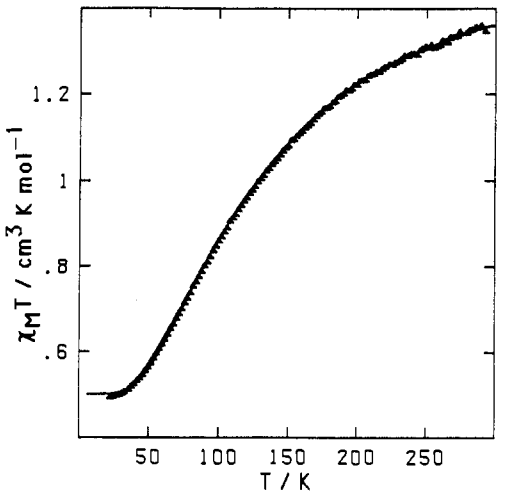

Figure 5. $\chi_M T$ versus T plot for [Ni(bapa)(H$_2$O)Cu(pba)]: (Δ) experimental points; (—) calculated curve.

minimum around 3900 G. No new transition is observed when the temperature is increased. This envelope is likely associated with the low-lying Kramers doublets arising from the quartet ground state. This spectrum is much less resolved than that obtained with the previously described NiCuNi trinuclear species involving the Me$_6$-[14]ane-N$_4$ terminal ligand, which might have two origins: (i) it could be due to dipolar interactions arising from rather short Cu···Ni1 and Cu···Ni2 intermolecular separations, equal to 5.514 and 5.349 Å, respectively; (ii) the EPR spectrum could be associated with the electronic states of the chain resulting from the stacking of the trinuclear units along the *a* axis. Each trinuclear unit is hydrogen bonded to its neighbors through the water molecule of the nickel coordination sphere and the oxygen atoms of the oxamido bridging ligand. The very weak interactions between the trinuclear units due to this chain structure are not detected from the magnetic susceptibility data, but it is well established that the EPR spectra are much more sensitive to weak intermolecular interactions than the susceptibility data.[20]

[NiCu]. The $\chi_M T$ versus T plot for this compound is shown in Figure 5. At 290 K, $\chi_M T$ is equal to 1.36 cm^3 K mol^{-1}, then decreases continuously upon cooling and finally reaches a plateau below about 10 K with $\chi_M T$ = 0.50 cm^3 K mol^{-1}. This behavior

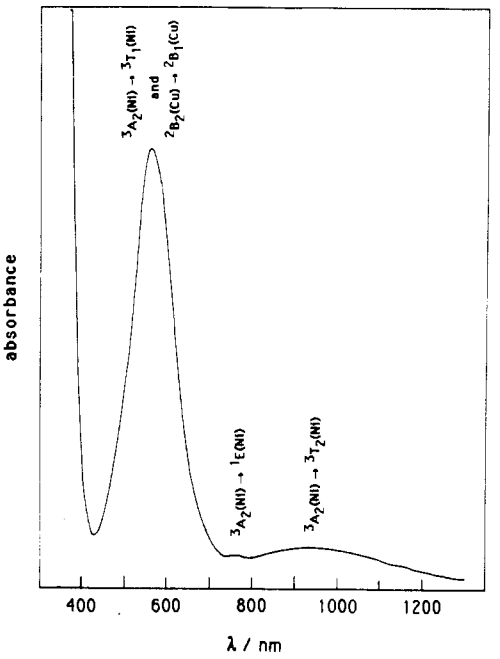

Figure 6. Electronic spectrum of {[Ni(bapa)(H$_2$O)]$_2$Cu(pba)}(ClO$_4$)$_2$ in acetonitrile solution.

is typical of an antiferromagnetically coupled Ni(II)Cu(II) pair with a doublet ground state and a quartet excited state located at an energy $-3J/2$ above.[3] The plateau corresponds to the temperature range where only the doublet ground state is thermally populated. The theoretical expression of $\chi_M T$ for such a compound is

$$\chi_M T = (N\beta^2/4k) \times \left[g_{1/2}^2 + 10g_{3/2}^2 \exp(3J/2kT)\right] / \left[1 + 2\exp(3J/2kT)\right] \quad (6)$$

where $g_{1/2}$ and $g_{3/2}$ are the g factors associated with the doublet and the quartet states, respectively. $g_{1/2}$ and $g_{3/2}$ are related to the local g factors g_{Ni} and g_{Cu}, assumed to be isotropic, through[3,18,19]

$$g_{1/2} = (4g_{Ni} - g_{Cu})/3$$
$$g_{3/2} = (2g_{Ni} + g_{Cu})/3 \quad (7)$$

Least-squares fitting of the magnetic data leads to J = −94.6 cm^{-1}, g_{Cu} = 2.02, and g_{Ni} = 2.24. The R agreement factor is then equal to 2.7 × 10^{-5}.

Electronic Spectrum of [NiCuNi]

The electronic spectrum for [NiCuNi] is shown in Figure 6. It exhibits three bands: (i) The first is an intense one (ϵ = 156 l cm^{-1} mol^{-1}) at 560 nm. This band is the envelope of two spin-allowed transitions, the $^3A_2$(Ni) → $^3T_1$(Ni) and the $^2B_2$(Cu) → $^2B_1$(Cu), using the O and D_2 site symmetries, respectively. The $^2B_2$(Cu) → $^2B_1$(Cu) band in the precursor Na$_2$Cu(pba) is found at 564 nm. (ii) The second is a weak and rather narrow band at 760 nm (ϵ = 12 l cm^{-1} mol^{-1}) assigned to the spin-forbidden transition $^3A_2$(Ni) → ^1E(Ni) activated by an exchange mechanism.[21,22] (iii) The third is a weak and broad band in the near-infrared region (ϵ = 15 l cm^{-1} mol^{-1}) corresponding to the $^3A_2$(Ni) → $^3T_2$(Ni) transition. The third spin-allowed transition for the nickel(II) chromophore $^3A_2$(Ni) → $^3T_2$(Ni), expected in the near-UV region, is hidden by a charge-transfer band due to the copper(II) chromophore.

Conclusion

{[Ni(bapa)(H$_2$O)]$_2$Cu(pba)]}(ClO$_4$)$_2$ is the first ABA trinuclear compound presenting an irregular spin state structure for which

(20) Journaux, Y.; Kahn, O.; Morgenstern-Badarau, I.; Galy, J.; Jaud, J.; Bencini, A.; Gatteschi, D. *J. Am. Chem. Soc.* **1985**, *107*, 6305.

(21) Güdel, H. In *Magneto-Structural Correlation in Exchange Coupled Systems*; Willett, R. D., Gatteschi, D., Kahn, O., Eds.; D. Reidel: Dordrecht, The Netherlands, 1985; p 297.

(22) Güdel, H. *Coord. Chem. Rev.* **1988**, *88*, 69.

Table IV. Relation between the Temperature T_{min} of the Minimum of $\chi_M T$ and the Isotropic Interaction Parameter J for an ABA Trinuclear Species with $S_B = {}^1/_2$ and Various Values of S_A (See Text)

S_A	1	${}^3/_2$	2	${}^5/_2$
$kT_{min}/\|J\|$	0.6435	1.420	2.131	3.374

the crystal structure has been solved. Its magnetic properties display characteristic signature of this kind of polymetallic systems, namely a minimum in the $\chi_M T$ versus T plot. The temperature T_{min} of the minimum of $\chi_M T$ for an ACu(II)A trinuclear species with an irregular spin state structure allows a first estimation of the A–Cu interaction parameter J. The values of $kT_{min}/|J|$ for $S_A = 1$, ${}^3/_2$, 2, and ${}^5/_2$ are given in Table IV. These values are calculated in the approximation where the g_A and g_{Cu} local g factors are equal and the local anisotropy of the A ion is negligible. In the case of a $Ni^{II}Cu^{II}Ni^{II}$ compound, the magnetic curve is weakly contrasted, the highest and lowest values of $\chi_M T$ being close to each other (2.31 and 2.03 cm^3 K mol^{-1} for [NiCuNi]). It follows that the parameters of the spin Hamiltonian cannot be determined without a rather large uncertainty. The J value corresponding to the best fit ($J = -90.3$ cm^{-1}), however, is very close to that found in the binuclear species [NiCu] with the same environment for the metal ions and the same bridging network, which suggests that J in [NiCuNi] is known with a fairly good accuracy. This value J inspires two remarks: (i) Its magnitude confirms, if it was still necessary, the efficiency of the bisbidentate bridges such as oxamido in transmitting an antiferromagnetic interaction between magnetic centers rather far apart from each other.[23] In the present case, the average value of the Ni···Cu separation is 5.31 Å. (ii) The magnitude of the interaction, nevertheless, is less pronounced than that in {[Ni(Me$_6$-[14]ane-N$_4$)]$_2$Cu(pba)}(ClO$_4$)$_2$ where a J value of -124 cm^{-1} had been deduced from the magnetic susceptibility data. The crystal structure of this previously studied compound is not known. One can, however, anticipate that the copper environment is less distorted than in [NiCuNi]. As a matter of fact, the surprisingly strong distorsion of the CuN_2O_2 chromophore in [NiCuNi], from a square planar to a tetrahedral environment, could result from the asymmetry of the nickel coordination spheres, certainly more pronounced in [NiCuNi] than in {[Ni(Me$_6$-[14]ane-N$_4$)]$_2$Cu(pba)}(ClO$_4$)$_2$. If so, the weaker value of $|J|$ in [NiCuNi] would come from a less planar environment around the copper atom. It is, indeed, well established that, with this kind of compounds, the planarity of the bridging network favors the overlap of the magnetic orbitals.[23]

To conclude, we shall recall that the ferromagnetic-like polarization of high local spins owing to an antiferromagnetic interaction with a small local spin is one of the approaches that has led to the design of molecular-based compounds exhibiting a spontaneous magnetization.[24,25]

Acknowledgment. J.R., C.D., and R.C. are very grateful to the CICYT (Grant MAT88-0545) and the CIRIT (Generalitat of Catalunya) for their financial assistance.

Supplementary Material Available: Structure determination details (Table SI), H atom positions (Table SII), anisotropic thermal parameters (Table SIII), distances and angles in terminal ligands, anions, and H bonds (Table SIV), atom to mean-plane distances and dihedral angles (Table SV), and experimental and calculated $\chi_M T$ values for [NiCuNi] (Table SVI) (9 pages); a listing of structure factors for [NiCuNi] (24 pages). Ordering information is given on any current masthead page.

(23) Kahn, O. *Angew. Chem., Int. Ed. Engl.* **1985**, *24*, 834.
(24) Caneschi, A.; Gatteschi, D.; Renard, J. P.; Rey, P.; Sessoli, R. *J. Am. Chem. Soc.* **1989**, *111*, 785.
(25) Nakatani, K.; Carriat, J. Y.; Journaux, Y.; Kahn, O.; Llioret, F.; Renard, J. P.; Pei, Y.; Sletten, J.; Verdaguer, M. *J. Am. Chem. Soc.* **1989**, *111*, 5739.

Contribution from the Dipartimento di Chimica, Università di Sassari, Via Vienna 2, I-07100 Sassari, Italy, and Dipartimento di Chimica Inorganica, Chimica Fisica e Chimica dei Materiali, Università di Torino, Via Pietro Giuria 7, I-10125 Torino, Italy

Infrared Frequencies and Intensities of the Vibrational Modes of Alkynes Coordinated on Metal Carbonyl Clusters

Pier Luigi Stanghellini*,† and Rosanna Rossetti‡

Received July 19, 1989

Assignments are proposed for the main vibrational modes of an alkyne molecule coordinated to metal complexes. The modes are the C—H, CH_3, C≡C, and C—C stretchings and the C—H and CH_3 deformations of the bonded acetylene, propyne, and 2-butyne. Several model complexes are used, e.g. $Co_2(CO)_6(\mu_2,\eta^2$-alkyne), $Os_3(CO)_{10}(\mu_3,\eta^2$-alkyne), $Co_2Ru(\mu_3,\eta^2$-alkyne), $Co_4(CO)_{10}(\mu_4,\eta^2$-alkyne), and $Co_4(CO)_{10}(\mu_4$-S)$(\mu_4,\eta^2$-alkyne), where the alkyne coordination is schematically indicated as σ_2, $\sigma_2\pi$, $\sigma_2\pi_2$ and σ_4, respectively. The average frequency of the bands belonging to the same type of vibrations and the contribution per C–H bond to the total C–H stretching and bending intensities are evaluated and compared with the relevant values for the free alkyne. Both the frequency and intensity data provide informations on the effect induced in the alkyne (bond strengths and charge distributions) by the metal coordination and are related to the type of the metal–alkyne bond, to the nuclearity, and to the geometry of the cluster.

Introduction

The alkynes are peculiar ligands in organometallic complexes and are known to exhibit several bonding modes, depending on the number of metal centers to which they are coordinated and on the type of the bond itself, usually known as a σ or π bond, according to its symmetry.[1-3]

The coordination to the metals causes the well-known structural changes in the alkyne molecules, mainly the lengthening of the triple bond and the decreasing of the bond angle, both depending on the change of the electron density in the alkyne MO's. The relationship between the two structural parameters has been recently rationalized[4] and appears, as could be reasonably expected, to be especially due to the number of metal atoms to which the alkyne is coordinated.

Together with the structural modifications, the coordinated alkyne exhibits significant changes in its vibrational pattern, among which is the well-documented decrease of the frequency of the

†Università di Sassari.
‡Università di Torino.

(1) Sappa, E.; Tiripicchio, A.; Braunstein, P. *Coord. Chem. Rev.* **1985**, *65*, 219.
(2) Raithby, P. R.; Rosales, M. J. *Adv. Inorg. Chem. Radiochem.* **1985**, *29*, 169.
(3) Sappa, E.; Tiripicchio, A.; Braunstein, P. *Chem. Rev.* **1983**, *83*, 203.
(4) Gervasio, G.; Rossetti, R.; Stanghellini, P. L. *Organometallics* **1985**, *4*, 1612.

0020-1669/90/1329-2047$02.50/0 © 1990 American Chemical Society